Rhodium and Iridium Phosphinothiolato Complexes. Synthesis and Crystal Structures of Mononuclear [M(cod)(*S,P*-$SC_2B_{10}H_{10}PPh_2$)] and Dinuclear [$M_2(CO)_2$(*S,P*-μ-$SC_2B_{10}H_{10}PPh_2$)] (M = Rh, Ir) and Their Performance in Catalytic Carbonylation

Heung-Sae Lee,[†] Jin-Young Bae,[†] Dae-Hyun Kim,[†] Hoon Sik Kim,*[,‡] Sung-Joon Kim,[†] Sungil Cho,[§] Jaejung Ko,*[,†] and Sang Ook Kang*[,†]

Department of Chemistry, Korea University, 208 Seochang, Chochiwon, Chung-nam 339-700, Korea, Korea Institute of Science and Technology, P.O. Box 131, Cheongryangri, Seoul 130-650, Korea, and Department of Chemical Engineering, Junnong-dong 90, Seoul City University, Seoul 130-743, Korea

Received August 27, 2001

The synthesis of new group 9 metal complexes containing the P,S-chelate ligands *P,S*-[$SC_2B_{10}H_{10}(CH_2)_nPPh_2$] ($n$ = 0, Cab^{P,S} (**2a**); n = 1, Cab^{CH2P,S} (**2b**)) is described. Two new phosphinothiolato complexes of the type [M(Cab^{P,S})(cod)] (M = Rh (**3a**), Ir (**3b**); cod = 1,5-cyclooctadiene) have been synthesized by the reaction of chloride-bridged dimers [M(μ-Cl)(cod)]$_2$ with 2 mol equiv of the corresponding lithium phosphinothiolato ligand LiCab^{P,S} (**2a**). The X-ray crystal structure determination of **3** shows a mononuclear, square-planar *cis*-P,S metal complex with a cod ligand. Carbonylation of the cod complexes **3** yields the dinuclear complexes [M(μ-*S*-Cab^{P,S})(CO)]$_2$ (where M = Rh (**4a**), Ir (**4b**)). The molecular structures reveal that the two metal atoms are bridged by the two thiolato ligands, and the carbonyls complete the coordination of the metal atoms. Dinuclear complexes **4** were also formed upon reaction of carbonyl dimers [M(μ-Cl)(CO)$_2$]$_2$ with 2 equiv of **2a**. Addition reactions of the dinuclear complexes **4** with triethylphosphine give the monosubstituted mononuclear metal complexes [M(Cab^{P,S})(CO)(PEt_3)] (where M = Rh (**5a**), Ir (**5b**)), which are obtained as trans isomers. The molecular structure of complex **5a** has been determined by X-ray diffraction methods. In an analogous manner, reaction of **2b** with [Rh(CO)$_2$(acac)] (acac = acetylacetone) produces a dinuclear thiolato-bridged complex, [Rh(μ-*S*-Cab^{CH2P,S})(CO)]$_2$ (**6**). Complex **6** was characterized by single-crystal X-ray analysis. Reacting **6** with 2 equiv of PEt_3 gave the trans-phosphino P,S-chelate complex [Rh(Cab^{CH2P,S})(CO)(PEt_3)] (**7**), analogous to **5**. The mono- and dinuclear P,S-chelates **4** and **5** catalyze the carbonylation of methanol to acetic acid. In particular, the dinuclear rhodium carbonyl complex **4a** is much more effective in catalyzing the carbonylation of methanol to acetic acid than the previously known catalyst [$RhI_2(CO)_2$]$^-$.

Introduction

Interest in dinuclear metal complexes has increased in the past few years, due to the fact that the reactivity and properties of a metal may be strongly modified by the presence of another metallic center in close proximity. In fact, dinuclear metal complexes using sulfur-containing bridging ligands, such as thiolate,[1] aminothiolate,[2] and phosphinothiolate,[3] to hold two metal atoms in close proximity have received considerable attention in recent years. One of the main reasons is the interest in the cooperative influence[4] of neighboring metal centers on catalytic reactions. The design of new dinuclear metal complexes involves the use of a newly assembled P,S-chelating ligand[5] containing a bulky *o*-carborane backbone. Recent reports of unusually stable C,N-,[6] C,P-,[7] N,P-,[8] N,S-,[9] and S,S′-chelating[10] *o*-carboranylmetal complexes appear to imply that the

[†] Korea University.
[‡] Korea Institute of Science and Technology.
[§] Seoul City University.

(1) Diéguez, M.; Claver, C.; Masdeu-Bultó, Ruiz, A.; van Leeuwen, P. W. N. M.; Schoemaker, G. C. *Organometallics* **1999**, *18*, 2107 and references therein.
(2) (a) Polo, A.; Claver, C.; Castillón, S.; Ruiz, A.; Bayón, J. C.; Real, J.; Mealli, C.; Masi, D. *Organometallics* **1992**, *11*, 3525. (b) Polo, A.; Fernandez, E.; Claver, C.; Castillón, S. *J. Chem. Soc., Chem. Commun.* **1992**, 639. (c) Bayon, J. C.; Esteban, P.; Real, J.; Claver, C.; Ruiz, A. *J. Chem. Soc., Chem. Commun.* **1989**, 1056.
(3) Dilworth, J. R.; Miller, J. R.; Wheatly, N.; Baker, M. J.; Sunley, J. G. *J. Chem. Soc., Chem. Commun.* **1995**, 1579.
(4) (a) Bosnich, B. *Inorg. Chem.* **1999**, *38*, 2554. (b) Brost, R. D.; Fjeldsted, D. O. K.; Stobart, R. *J. Chem. Soc., Chem. Commun.* **1989**, 488. (c) Poilblanc, R. *Inorg. Chim. Acta* **1982**, *62*, 75.
(5) Teixidor, F.; Viòas, C.; Benakki, R.; Kivekäs, R.; Sillanpää, R. *Inorg. Chem.* **1997**, *36*, 1719.
(6) (a) Lee, J.-D.; Kim, S.-J.; Yoo, D.; Ko, J.; Cho, S.; Kang, S. O. *Organometallics* **2000**, *19*, 1695. (b) Bae, J.-Y.; Lee, Y.-J.; Kim, S.-J.; Ko, J.; Cho, S.; Kang, S. O. *Organometallics* **2000**, *19*, 1514. (c) Lee, J.-D.; Baek, C.-K.; Ko, J.; Park, K.; Cho, S.; Min, S.-K.; Kang, S. O. *Organometallics* **1999**, *18*, 2189.
(7) Lee, T.; Lee, S. W.; Jang, H. G.; Ko, J.; Kang, S. O. *Organometallics* **2001**, *20*, 741.
(8) Lee, H.-S.; Bae, J.-Y.; Ko, J.; Kang, Y. S.; Kim, H. S.; Kim, S.-J.; Chung, J.-H.; Kang, S. O. *J. Organomet. Chem.* **2000**, *614*−*615*, 83.
(9) Chung, S.-W.; Ko, J.; Park, K.; Cho, S.; Kang, S. O. *Collect. Czech. Chem. Commun.* **1999**, *64*, 883.

10.1021/om0107789 CCC: $22.00
Publication on Web 12/11/2001

Chart 1

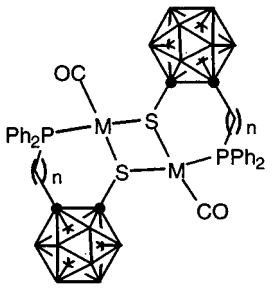

$[M_2(CO)_2(Cab^{P,S})]_2$
(M = Rh, n = 0 **4a**; M = Ir, n = 0 **4b**; M = Rh, n = 1 **6**)

chelation, rigid conformation, and *o*-carboranyl ligand backbone might be ideal for the stabilization of possible dinuclear metal intermediates for organometallic reactions. In addition, the long-term thermal stability of such metal complexes, which is essential for catalytic carbonylation of methanol, can be realized by incorporating a thermally robust *o*-carborane ligand backbone.

Our specific interests at this point are centered in dinuclear complexes of the type $[M(\mu\text{-}S\text{-}Cab^{P,S})(CO)]_2$ and $[M(\mu\text{-}S\text{-}Cab^{CH2P,S})(CO)]_2$ (M = Rh, Ir) with a P,S-chelating phosphinothiolato ligand such as *o*-$Cab^{P,S}$ (**2a**) and *o*-$Cab^{CH2P,S}$ (**2b**), as shown in Chart 1. The use of *o*-carborane as the ligand backbone is rare in catalytic reactions, while the *nido*-$\{C_2B_9\}$ complex has been proven to be a useful ancillary ligand for catalytic hydrogenation reactions.[11] This ligand **2** has been chosen because it has an arylphosphine at one end to stabilize the metal ion in a low oxidation state and a coordinating sulfur function at the other end which will readily be utilized as a bridging ligand by an incoming metal fragment to form a dinuclear metal complex.

To investigate the influence of the P,S-chelate ligand **2** on the catalytic behavior of the complex in the carbonylation reaction, we have synthesized and characterized the dinuclear rhodium and iridium complexes of general formula $[M(\mu\text{-}S\text{-}Cab^{P,S})(CO)]_2$ (where M = Rh (**4a**), Ir (**4b**)) and $[Rh(\mu\text{-}S\text{-}Cab^{CH2P,S})(CO)]_2$ (**6**). In particular, complex **4a** was successfully applied as a homogeneous catalyst for the carbonylation of methanol, and its catalytic activity is discussed.

Results and Discussion

Ligand Synthesis. Reaction of known *o*-carborane reagents such as $HCab^P$ (**1a**; $Hcab^P$ = *closo*-1-(diphenylphosphino)-*o*-carborane)[12] and $Hcab^{CH2P}$ (**1b**; $HCab^{CH2P}$ = *closo*-1-((diphenylphosphino)methyl)-*o*-carborane)[13] with 1.1 equiv of Bu^nLi, followed by the addition of 1 equiv of sulfur in THF at low temperature (Scheme 1), results in virtually quantitative formation of the corresponding lithium phosphinothiolates $LiCab^{P,S}$ (**2a**; $LiCab^{P,S}$ = *closo*-1-(diphenylphosphino)-2-(lithiumthiolato)-*o*-carborane) and $LiCab^{CH2P,S}$ (**2b**; $LiCab^{CH2P,S}$ = *closo*-1-((diphenylphosphino)methyl)-2-(lithiumthiolato)-*o*-carborane), respectively.

Scheme 1. Synthesis of the P,S-Chelating Ligand 2 (*n* = 0, a; *n* = 1, b)[a]

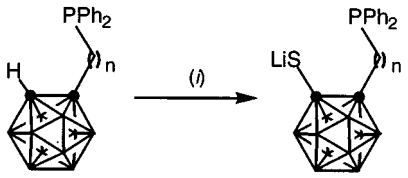

$HCab^{P,S}$ **1a** or $HCab^{CH2P,S}$ **1b** $LiCab^{P,S}$ **2a** or $LiCab^{CH2P,S}$ **2b**

[a] Legend: (*i*) (*a*) $LiBu^n$, THF, −78 °C; (*b*) S_8, THF, 25 °C.

Scheme 2. Synthesis of the P,S-Chelating Metal cod Complexes[a]

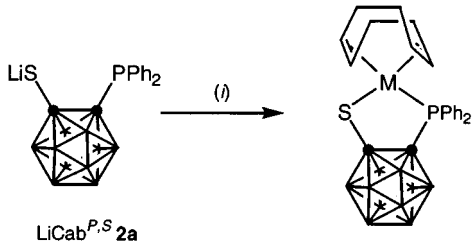

$LiCab^{P,S}$ **2a** $[M(Cab^{P,S})(cod)]$ **3**

[a] Legend: (*i*) $^1/_2[M(\mu\text{-Cl})(cod)]_2$ (M = Rh, Ir), THF, 25 °C.

Reaction of $LiCab^{P,S}$ (2a) with $[M(\mu\text{-Cl})(cod)]_2$ (M = Rh, Ir; cod = Cycloocta-1,5-diene). P,S-Chelated phosphinothiolato metal complexes, $[M(Cab^{P,S})(cod)]$ (**3**), were prepared by reactions between the dimeric metal complexes and 2 equiv of the corresponding lithium phosphinothiolate **2a** (Scheme 2).

Isolation of pure products, which ranged in color from yellow to orange, was achieved by recrystallization. Typically, the yields of **3** were on the order of 79−86%. Elemental analysis results show that the air-stable complexes **3** have compositions corresponding to a 1:1 metal complex of the M(cod) fragment and phosphinothiolato ligand **2a**. Complexes **3** were further characterized by IR and NMR (^1H, ^{13}C, and ^{31}P) spectra. The ^1H NMR spectra of **3** show signals for the cyclooctadiene ligand at around δ 2.2−3.0 (methylene protons) and 5.0−5.3 (olefinic protons). The diphenylphosphine moiety exhibits multiplets at around δ 7.1−8.1, assigned

(10) (a) Kim, D.-H.; Ko, J.; Park, K.; Cho, S.; Kang, S. O. *Organometallics* **1999**, *18*, 2738. (b) Bae, J.-Y.; Park, Y.-I.; Ko, J.; Park, K.-I.; Cho, S.-I.; Kang, S. O. *Inorg. Chim. Acta* **1999**, *289*, 141.

(11) (a) Viñas, C.; Flores, M. A.; Núñez, R.; Teixidor, F.; Kivekäs, R.; Sillanpää, R. *Organometallics* **1998**, *17*, 2278. (b) Texidor, F.; Flores, M. A.; Viñas, C.; Kivekäs, R.; Sillanpää, R. *Angew. Chem., Int. Ed. Engl.* **1996**, *35*, 2251. (c) Pirotte, B.; Felekidis, A.; Fontaine, M.; Demonceau, A.; Noels, A. F.; Delarge, J.; Chizhevsky, I. T.; Zinevich, T. V.; Pisareva, I. V.; Bregadze, V. I. *Tetrahedron Lett.* **1993**, *34*, 1471. (d) Belmont, J. A.; Soto, J.; King, R. E., III; Donaldson, A. J.; Hewes, J. D.; Hawthorne, M. F. *J. Am. Chem. Soc.* **1989**, *111*, 7475. (e) Behnken, P. E.; Belmont, J. A.; Busby, D. C.; Delaney, M. S.; King, R. E., III; Kreimendahl, C. W.; Marder, T. B.; Wilczynski, J. J.; Hawthorne, M. F. *J. Am. Chem. Soc.* **1984**, *106*, 3011. (f) Behnken, P. E.; Busby, D. C.; Delaney, M. S.; King, R. E., III; Kreimendahl, C. W.; Marder, T. B.; Wilczynski, J. J.; Hawthorne, M. F. *J. Am. Chem. Soc.* **1984**, *106*, 7444. (g) Paxson, T. E.; Hawthorne, M. F. *J. Am. Chem. Soc.* **1974**, *96*, 4674.

(12) Hill, W. E.; Silva-Trivino, L. M. *Inorg. Chem.* **1979**, *18*, 361.

(13) Zakharkin, L. I.; Zhubekova, M. N.; Kazantsev, A. V. *Zh. Obshch. Khim.* **1972**, *42*, 1024.

Table 1. X-ray Crystallographic Data and Processing Parameters for Compounds 3a, 3b, 4a·(hexane), 4b, 5a, and 6·4THF

	3a	**3b**	**4a**·(hexane)	**4b**	**5a**	**6**·4THF
formula	$B_{10}C_{22}H_{32}PSRh$	$B_{10}C_{22}H_{32}PSIr$	$B_{20}C_{36}H_{54}O_2P_2S_2Rh_2$	$B_{20}C_{30}H_{40}O_2P_2S_2Ir_2$	$B_{10}C_{21}H_{35}OP_2SRh$	$B_{20}C_{48}H_{76}O_6P_2S_2Rh_2$
fw	570.52	659.81	1066.93	1159.28	608.50	1297.24
cryst class	monoclinic	monoclinic	monoclinic	monoclinic	monoclinic	monoclinic
space group	$P2_1/n$	$P2_1/n$	$P2_1/c$	$P2_1/c$	$P2_1/n$	$C2/c$
Z	4	4	4	4	4	8
cell constants						
a, Å	12.6713(1)	12.687(1)	14.633(2)	14.8970(1)	11.6078(6)	14.7620(7)
b, Å	11.114(2)	11.1010(6)	30.160(2)	29.9518(2)	21.9130(1)	16.5850(7)
c, Å	18.743(3)	18.741(1)	10.8636(9)	10.8565(8)	11.6386(8)	25.9780(7)
V, Å^3	2606.6(7)	2604.3(3)	4790.1(9)	4837.7(6)	2939.3(3)	6353.1(4)
β, deg	99.06(1)	99.366(6)	92.414(9)	92.945(7)	96.846(5)	92.688(2)
μ, cm^{-1}	8.09	52.81	8.75	56.76	7.76	6.78
cryst size, mm	0.25 × 0.3 × 0.3	0.1 × 0.25 × 0.4	0.2 × 0.2 × 0.4	0.2 × 0.25 × 0.25	0.2 × 0.2 × 0.3	0.35 × 0.35 × 0.35
D_{calcd}, g/cm^3	1.454	1.683	1.479	1.592	1.375	1.356
F(000)	1160	1288	2048	2208	1240	2528
radiation	Mo Kα (λ = 7170 Å)					
θ range, deg	1.82−25.98	1.81−25.97	1.35−25.97	1.36−25.97	1.86−25.97	1.57−21.08
h, k, l collected	+15, +13, ±23	+15, +13, ±23	±18, +37, +13	±18, +37, +13	+14, +27, ±14	+14, ±16, ±26
no. of rflns collected/ unique	3322/3264	5376/5101	9927/9374	9585/9095	6100/5774	3440/3440
no. of data/restraints/ params	3264/0/336	5101/0/336	9374/0/579	9095/0/563	5774/0/348	3440/0/331
goodness of fit on F^2	0.864	0.703	0.997	1.174	0.943	1.396
final R indices ($I > 2\sigma(I)$)[a]						
R1	0.0279	0.0235	0.0689	0.0506	0.0494	0.0551
wR2	0.0908	0.0733	0.1531	0.1429	0.1264	0.1641
R indices (all data)						
R1	0.0421	0.0373	0.1995	0.1143,	0.1230	0.0679
wR2	0.1040	0.0861	0.2063	0.1830	0.1622	0.1810

[a] R1 = $\sum||F_o| - |F_c||$ (based on reflections with $F_o^2 > 2\sigma F^2$). wR2 = $[\sum[w(F_o^2 - F_c^2)^2]/\sum[w(F_o^2)^2]]^{1/2}$; $w = 1/[\sigma^2(F_o^2) + (0.095P)^2]$; $P = [\max(F_o^2, 0) + 2F_c^2]/3$ (also with $F_o^2 > 2\sigma F^2$).

to the phenyl groups. The IR spectra of **3** exhibit one ν(C═C) stretching band at about 1437−1439 cm^{-1} and an intense B−H stretch at about 2560−2606 cm^{-1}. In particular, the $^{31}P\{^1H\}$ NMR of **3a** spectrum shows a doublet with a $^1J_{Rh-P}$ value of 169 Hz, corresponding to the $-PPh_2$ group of the phosphinothiolate ligand. The above spectral data suggest that the P,S-chelates **3** have the structure shown in Scheme 2. Confirmation of this structure came from a single-crystal X-ray structure determination.

The molecular structure of **3a** is shown in Figure 1, and listings of selected bond lengths and angles for **3a** can be found in Tables 2 and 3, respectively. The crystal structure shows that coordination around the rhodium atom is approximately square planar. The carborane cage is coordinated bidentately through P and S atoms to the Rh(I) ion, while cod is η^4-coordinated to the metal. Both the Rh−S and Rh−P bond lengths at 2.295(1) and 2.2615(9) Å are typical,[14] but Rh−(C_{15},C_{16}) and Rh−(C_{19},C_{20}) differ significantly due to the stronger trans influence of the phosphorus versus sulfur. The cyclopentadienyl ring exhibits a boat conformation, with Rh−C and C−C bond distances within the normal range for Rh(I)−cod complexes.[15] The five-membered Rh−S−C−C−P ring is essentially planar, with no deviation from the least-squares plane of more than 0.093 Å. The sum of the angles (360.01°) around Rh formed by the coordinated P and S atoms and the midpoints of the double-bond carbon atoms of cod indicate the planarity of the (*P*,*S*)Rh(diene) moiety. The bond lengths and angles associated with cod and the coordinated phosphinothiolato ligand in **2a** are unexceptional with respect to those of other *o*-carborane-substituted compounds.

The molecular structure of **3b**, determined by an X-ray diffraction study, is shown in Figure 2. The structure has a strong resemblance to that of **3a**. The crystal structure shows that coordination around the iridium atom is approximately square planar. Selected

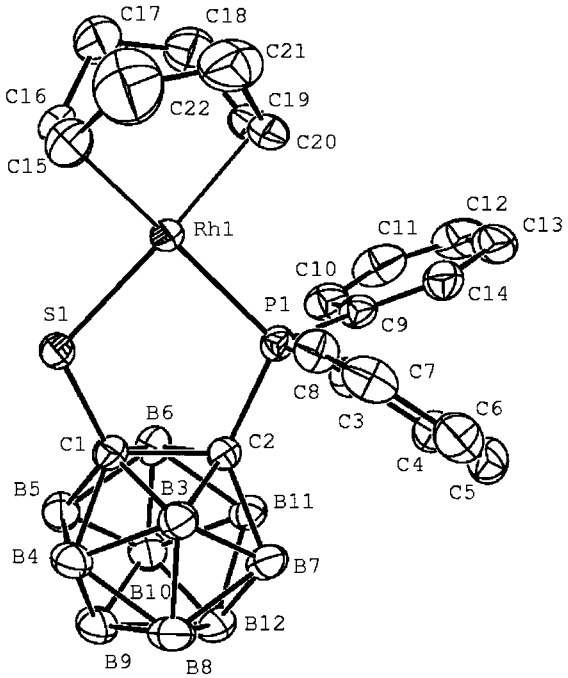

Figure 1. Molecular structure of **3a** with atom labeling. Ellipsoids show 30% probability levels; the unlabeled atoms are carbon atoms, and hydrogen atoms have been omitted for clarity.

(14) Dick, D. G.; Stephan, D. W. *Can. J. Chem.* **1986**, *64*, 1870.
(15) (a) Pinillos, M. T.; Jarauta, M. P.; Elduque, A.; Lahoz, F. J.; Oro, L. A. *J. Organomet. Chem.* **1996**, *514*, 119. (b) Calvo, M. A.; Manotti Lanfredi, A. M.; Oro, L. A.; Pinillos, M. T.; Tejel, C.; Tiripicchio, A.; Ugozzoli, F. *Inorg. Chem.* **1993**, *32*, 1147.

Table 2. Selected Interatomic Distances (Å) in 3a, 3b, 4a·(hexane), 4b, 5a, and 6·4THF

			Compound **3a**				
Rh(1)−C(19)	2.154(5)	Rh(1)−C(20)	2.161(6)	Rh(1)−C(15)	2.216(5)	Rh(1)−S(1)	2.295(1)
Rh(1)−C(16)	2.257(3)	Rh(1)−P(1)	2.2615(9)				
			Compound **3b**				
Ir(1)−C(15)	2.145(5)	Ir(1)−C(16)	2.152(5)	Ir(1)−C(20)	2.193(5)	Ir(1)−S(1)	2.285(1)
Ir(1)−C(19)	2.238(5)	Ir(1)−P(1)	2.267(1)				
			Compound **4a**·(hexane)				
Rh(1)−C(15)	1.83(1)	O(1)−C(15)	1.17(1)	Rh(1′)-S(1′)	2.343(3)	Rh(1′)-C(15′)	1.84(1)
Rh(1)−S(1′)	2.388(3)	Rh(1)−P(1)	2.224(3)	O(1′)-C(15′)	1.16(1)	Rh(1′)-S(1)	2.398(2)
Rh(1′)-P(1′)	2.225(3)	Rh(1)−Rh(1′)	2.980(1)	Rh(1)−S(1)	2.349(3)		
			Compound **4b**				
Ir(1)−C(15)	1.80(2)	O(1)−C(15)	1.19(2)	Ir(1′)-S(1′)	2.368(3)	Ir(1′)-C(15′)	1.84(1)
Ir(1)−S(1′)	2.435(3)	Ir(1)−P(1)	2.261(3)	O(1′)-C(15′)	1.14(2)	Ir(1′)-S(1)	2.429(3)
Ir(1′)-P(1′)	2.261(3)	Ir(1)−Ir(1′)	2.9991(7)	Ir(1)−S(1)	2.363(3)		
			Compound **5a**				
Rh(1)−C(15)	1.810(8)	Rh(1)−P(1)	2.298(1)	O(1)−C(15)	1.152(9)	Rh(1)−P(2)	2.317(2)
Rh(1)−S(1)	2.34(2)						
			Compound **6**·4THF				
Rh(1)−C(16)	1.826(9)	Rh(1)−P(1)	2.243(2)	C(16)−O(1)	1.14(1)	Rh(1)−S(1)*	2.383(2)
Rh(1)−S(1)	2.388(2)						

Table 3. Selected Interatomic Angles (deg) in 3a, 3b, 4a·(hexane), 4b, 5a, and 6·4THF

			Compound **3a**				
P(1)−Rh(1)−S(1)	89.33(4)	C(1)−S(1)−Rh(1)	108.7(1)	C(3)−P(1)−Rh(1)	113.9(1)	C(9)−P(1)−Rh(1)	114.8(1)
C(1)−C(2)−P(1)	110.5(3)	C(2)−P(1)−Rh(1)	110.8(1)	C(2)−C(1)−S(1)	118.5(3)		
			Compound **3b**				
P(1)−Ir(1)−S(1)	90.16(4)	C(9)−P(1)−Ir(1)	114.6(1)	C(1)−C(2)−P(1)	110.7(3)	C(3)−P(1)−Ir(1)	114.3(2)
C(2)−C(1)−S(1)	119.0(3)	C(2)−P(1)−Ir(1)	109.9(1)	C(1)−S(1)−Ir(1)	108.2(2)		
			Compound **4a**·(hexane)				
P(1)−Rh(1)−S(1)	91.04(9)	Rh(1′)−S(1′)−Rh(1)	78.06(8)	S(1′)−Rh(1′)−S(1)	78.19(8)	C(15′)−Rh(1′)−P(1′)	87.6(3)
S(1)−Rh(1)−S(1′)	78.29(9)	C(15)−Rh(1)−P(1)	87.5(3)	C(15)−Rh(1)−S(1′)	103.2(3)	Rh(1)−S(1)−Rh(1′)	77.74(8)
C(15′)−Rh(1′)−S(1)	103.4(3)	P(1′)−Rh(1′)−S(1′)	91.18(9)				
			Compound **4b**				
P(1)−Ir(1)−S(1)	90.9(1)	Ir(1′)−S(1′)−Ir(1)	77.27(9)	S(1′)−Ir(1′)−S(1)	78.9(1)	C(15′)−Ir(1′)−P(1′)	88.2(4)
S(1)−Ir(1)−S(1′)	78.8(1)	C(15)−Ir(1)−P(1)	88.3(5)	C(15)−Ir(1)−S(1′)	102.3(5)	Ir(1)−S(1)−Ir(1′)	77.47(9)
C(15′)−Ir(1′)−S(1)	102.2(4)	P(1′)−Ir(1′)−S(1′)	90.8(1)				
			Compound **5a**				
C(15)−Rh(1)−P(1)	93.7(2)	P(2)−Rh(1)−S(1)	86.56(7)	C(15)−Rh(1)−P(2)	92.7(2)	P(1)−Rh(1)−S(1)	87.04(5)
			Compound **6**·4THF				
C(16)−Rh(1)−P(1)	87.1(2)	C(1)−S(1)−Rh(1)	113.6(2)	Rh(1)*-S(1)−Rh(1)	93.78(6)	P(1)−Rh(1)−S(1)	95.01(6)
S(1)*-Rh(1)−S(1)	78.44(6)	C(16)−Rh(1)−S(1)*	98.2(2)	C(2)−C(3)−P(1)	118.1(5)	C(3)−P(1)−Rh(1)	112.5(2)

bond lengths and angles for **3b** are listed in Table 2. The Ir−P bond length of 2.267(1) Å lies within the usual range for a dative bond between the iridium and phosphorus atom,[16] which typically ranges from 2.2 to 2.30 Å, depending on the coordination number of the Ir atom. The iridium−sulfur bond length of 2.285(1) Å is somewhat shorter than that observed for other monomeric thiolate complexes such as [Ir(SC_6H_3Me-2,6)(CO)-(PPh_3)$_2$] (2.393(2) Å).[17] In Table 2, the Ir−C(cod) distance trans to C−S averages 2.149(5) Å. In contrast, the average Ir−C(cod) distance trans to C−PPh_2 is 2.216-(5) Å. Thus, the Ir−C(cod) distance trans to C−S is approximately 0.07 Å shorter than that trans to C−PPh_2. The more extensive the back-donation, the shorter will be the Ir−alkene distance found in the alkene fragment trans to C−S.

Synthesis and Spectrosopic Characterization of Dinuclear Metal Complexes [M(Cab^{P,S})(CO)]$_2$ (M = Rh (4a), Ir (4b)). The reaction of **3** with excess carbon monoxide occurs rapidly at room temperature to yield the dinuclear P,S-chelate metal complexes [M(μ-*S*-Cab^{P,S})(CO)]$_2$ (M = Rh (**4a**), Ir (**4b**)), as shown in Scheme 3. Thus, carbon monoxide easily replaces the cod in complexes **3** to give the orange dinuclear metal complexes **4** in excellent yields.

Complexes **4** were isolated as air-stable microcrystalline solids and were spectroscopically characterized. The composition of the new complexes **4** was unequivocally established by elemental analysis. Furthermore, the spectroscopic data (^{1}H, ^{13}C, and ^{31}P NMR) associated with **4** are also consistent with their assigned structures. The pattern and relative intensity of the ν(CO) bands of **4** resemble closely those of the dinuclear metal carbonyl thiolates having *trans*-dicarbonyl dirhodium environments.[17] In fact, complexes **4a** and **4b** exhibit one ν(CO) band at 1994 and 1985 cm^{-1}, respectively. The lower frequency shift of CO stretches in **4** as compared to those of the other carbonylmetal phosphinothiolates is indicative of a higher basicity in the Cab^{P,S} case. The ^{31}P{^{1}H} NMR spectrum of **4a** contained a doublet at δ 81.44 with $^1J_{Rh-P}$ = 169 Hz, consistent with

(16) (a) El Amane, M.; Maisonnat, A.; Dahan, F.; Prince, R.; Poilblanc, R. *Organometallics* **1985**, *4*, 773. (b) Pinillos, M. T.; Elduque, A.; Lopez, J. A.; Lahoz, F.; Oro, L. A. *J. Chem. Soc., Dalton Trans.* **1991**, 391. (c) Claver, C.; Kalck, Ph.; Fis, J.; Jaud, J. *Inorg. Chem.* **1987**, *26*, 3479.

(17) Dilworth, J. R.; Morales, D.; Zheng, Y. *J. Chem. Soc., Dalton Trans.* **2000**, 3007.

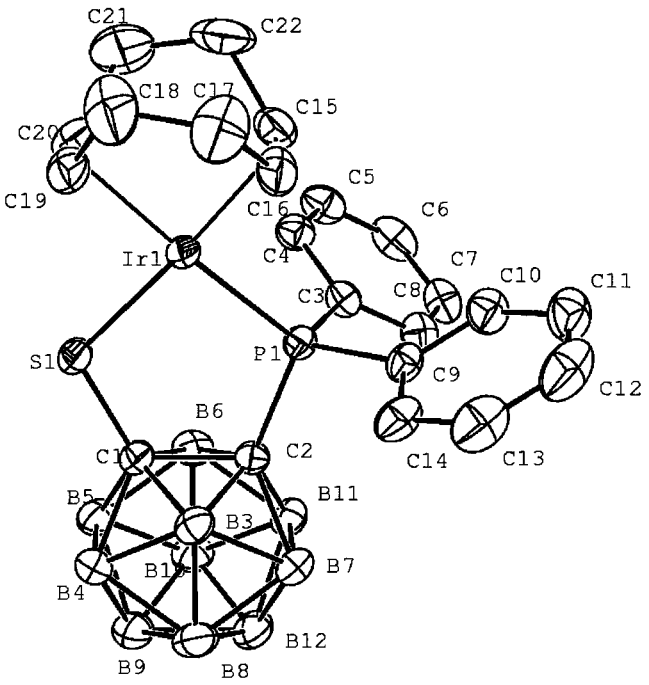

Figure 2. Molecular structure of **3b** with atom labeling. Ellipsoids show 30% probability levels; the unlabeled atoms are carbon atoms, and hydrogen atoms have been omitted for clarity.

Scheme 3. Synthesis of the Dinuclear P,S-Chelating Metal Carbonyl Complexes[a]

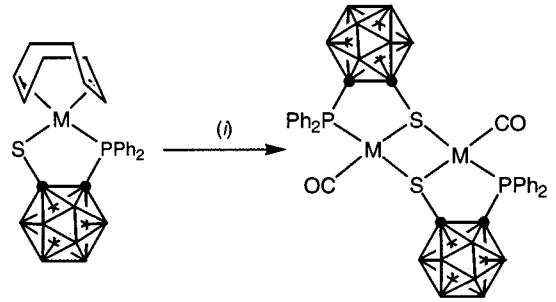

[M(Cab^{P,S})(cod)] **3** [M(Cab^{P,S})(CO)]$_2$ **4**

[a] Legend: (*i*) CO bubbling, toluene, 25 °C.

the phosphorus atom being in a chelate and in a trans position with respect to a sulfur donor atom.

The X-ray structure determination of **4a** was carried out, and the resulting ORTEP plot is shown in Figure 3. It consists of discrete dinuclear units possessing a center of symmetry at the midpoint of the Rh(1)−Rh(1)′ vector, which forms an Rh_2S_2 butterfly core with a thiolate bridge. Each Rh atom is four-coordinate and displays a square-planar geometry. There are a number of structures containing the Rh_2S_2 motif,[18] but to the best of our knowledge, this is the first dinuclear Rh(I) structure possessing an *o*-carboranyl thiolato ligand. Structural data for **4a** show that the two phosphinothiolate ligands act as thiolate bridges between the metal atoms, giving a hinged central Rh_2S_2 ring, as shown in Chart 2. When both bridging groups are connected to the bulky *o*-carboranyl unit, there is a significant distortion from planarity with a value of $\theta = 108.23°$ for the complex **4a**. Therefore, the folding along the S−S axis imposes shorter M−M distances (for instance, Rh−Rh = 2.980 Å in **4a**), although they are still too long to consider metal−metal interactions in these species. This distance is closer to dinuclear Rh(I) analogues (2.9−3.4 Å).[2a,3,18d,g−i]

The Rh_2S_2 ring is puckered, the dihedral angle between the planes defined by [Rh(1),S(1),Rh(1)′] and [Rh(1),S(1)′,Rh(1)′] being 71.57(7)°. The five-membered Rh−S−C−C−P ring is planar, with the dihedral angles between the planes defined by [Rh(1),P(1),C(1),C(2),S(1)]/[Rh(1)′,P(1)′,C(1)′,C(2)′,S(1)′] and [Rh(1),S(1),Rh(1)′]/[Rh(1)′,S(1)′,Rh(1)] being 58.3(1) and 58.8(1)°, respectively. The Rh−S distances (2.346(3) (average) and 2.393(3) (average) Å) are very similar to those observed for *anti*-[Rh_2-(μ-SBu^t)$_2$(CO)$_2$(PPh$_3$)$_2$] (2.357(1) and 2.391(6) Å)[19] and [Rh_2(μ-SPh)$_2$(CO)$_2$(PPh$_3$)$_2$] (2.375(7) and 2.400(7) Å).[20]

The molecular structure of **4b** is shown in Figure 4, and the most significant intramolecular bond lengths and angles are listed in Table 2. The structure has a strong resemblance to that of **4a**. The geometry around each iridium atom is typically square planar for such dinuclear bridged d^8 metal complexes.[20,21] Each iridium is bonded to two sulfur atoms of thiolato groups, one phosphorus atom of a phosphinothiolato ligand, and one carbon atom of a carbonyl group. The dihedral angle θ between the two square planes is 108.00(2)°, and the Ir−Ir distance is 2.999(7) Å. These values, expected from dinuclear d^8 complexes, correlate well with related dinuclear iridium complexes.[22]

Alternatively, such complexes **4** can be synthesized using a second route. When the compounds [M(μ-Cl)(CO)$_2$]$_2$ (M = Rh, Ir) were reacted with 2 equiv of **2a**, the dinuclear metal complexes **4** were obtained in good yield yields (66−78%), as shown in Scheme 4.

Ligand Substitutions of 4. To test the lability of Cab^{P,S} complexes of rhodium and iridium, and the stability of dinuclear complexes, the P,S-chelates **4** were allowed to react with triethylphosphine. Such complexes **4** react with an excess of PEt_3 to yield the corresponding mononuclear metal chelates *trans*-[M(Cab^{P,S})(CO)(PEt$_3$)] (M = Rh (**5a**), Ir (**5b**)), as shown in Scheme 5.

The phosphorus NMR spectra of **5a** exhibit sharp signals at δ 82.21, corresponding to the $-PPh_2$ group of the phosphinothiolate ligand, and at δ 26.22, corresponding to the PEt_3 ligand. The coupling constant $^2J_{PP}$ = 294 Hz is typical of a trans-P,P arrangement that places the bulky PPh_2 and PEt_3 groups away from each other. The ν(CO) frequency for **5** was found at lower

(18) (a) Hauptmann, E.; Shapiro, R.; Marshall, W. *Organometallics* **1998**, *17*, 4976. (b) Ciriano, M. A.; Perez-Torrente, J. J.; Lahoz, F. J.; Oro, L. A. *J. Organomet. Chem*. **1994**, *482*, 53. (c) Elduque, A.; Oro, L. A.; Pinillos, M. T.; Tiripicchio, A.; Ugozzoli, F. *J. Chem. Soc., Dalton Trans*. **1994**, 385. (d) Masdeu, A. M.; Ruiz, A.; Castillon, S.; Claver, C.; Hitchcock, P. B.; Chaloner, P. A.; Bo, C.; Poblet, J. M.; Sarasa, P. J. *J. Chem. Soc., Dalton Trans*. **1993**, 2689. (e) Jones, W. D.; Chin, R. M. *J. Am. Chem. Soc*. **1992**, *114*, 9851. (f) Bishop, P. T.; Dilworth, J. R.; Nicholson, T.; Zubieta, J. *J. Chem. Soc., Dalton Trans*. **1991**, 385. (g) Cruz-Garritz, D.; Garcia-Alejandre, J.; Torrens, H.; Alvarez, C.; Toscano, R. A.; Poilblanc, R.; Thorez, A. *Transition Met. Chem*. **1991**, *16*, 130. (h) Choukroun, R.; Dahan, F.; Gervais, D.; Rifai, C. *Organometallics* **1990**, *9*, 1982. (i) Hou, Z.; Ozawa, Y.; Isobe, K. *Chem. Lett*. **1990**, 1863.

(19) Jones, R. A.; Achwab, S. T. *J. Cryst. Struct. Res*. **1986**, *16*, 577.

(20) Bonnet, J. J.; Kalck, P.; Poilblanc, R. *Inorg. Chem*. **1977**, *16*, 1514.

(21) Bonnet, J. J.; Jeannin, Y.; Kalck, P.; Maisonnat, A.; Poilblanc, R. *Inorg. Chem*. **1975**, *14*, 743.

(22) (a) Bonnet, J. J.; Thorez, A.; Maisonnat, A.; Galy, J.; Poilblanc, R. *J. Am. Chem. Soc*. **1979**, *101*, 5940. (b) Bonnet, J. J.; Galy, J.; de Montauzon, D.; Poilblanc, R. *J. Chem. Soc., Chem. Commun*. **1977**, 47.

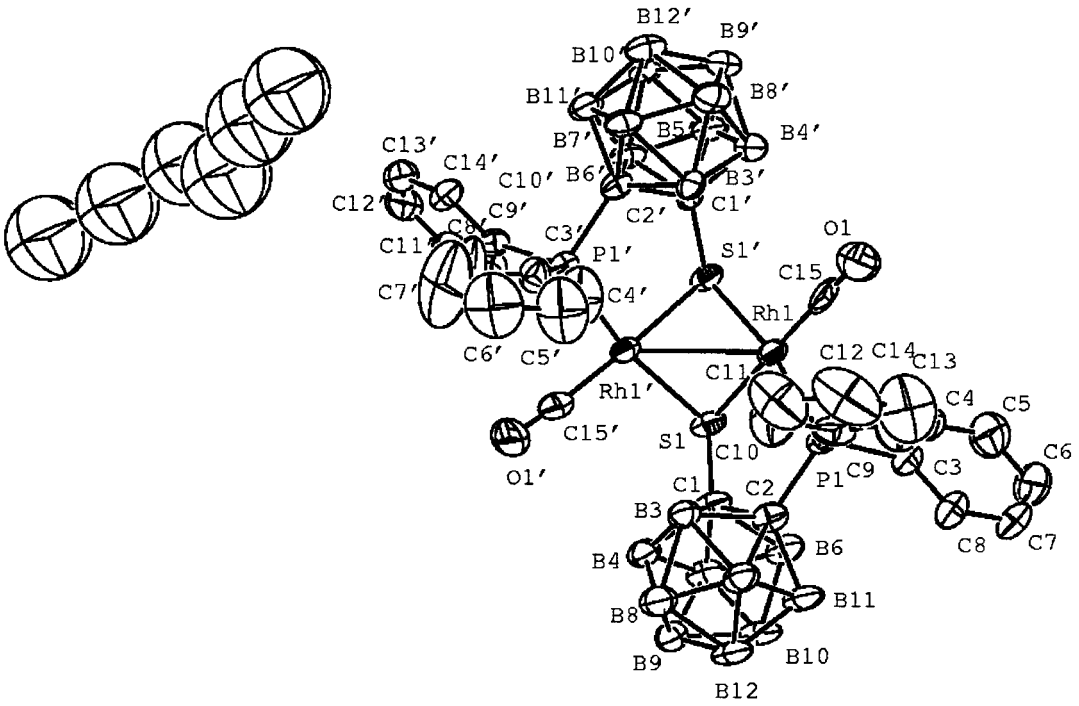

Figure 3. Molecular structure of **4a**·(hexane) with atom labeling. Ellipsoids show 30% probability levels; the unlabeled atoms are carbon atoms, and hydrogen atoms have been omitted for clarity.

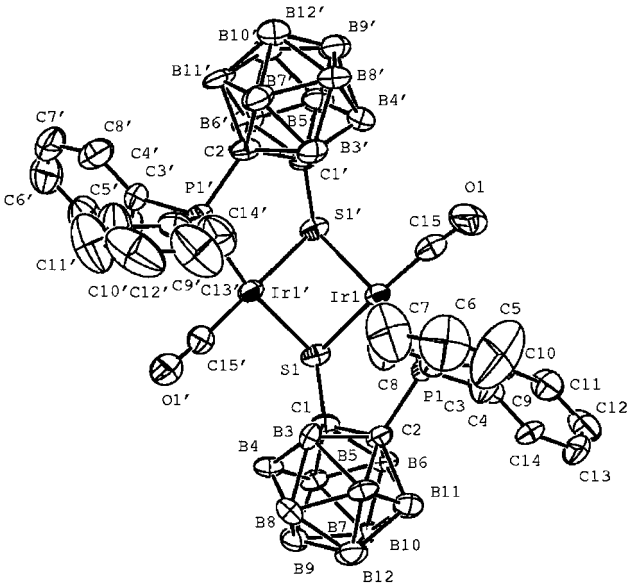

Figure 4. Molecular structure of **4b** with atom labeling. Ellipsoids show 30% probability levels; the unlabeled atoms are carbon atoms, and hydrogen atoms have been omitted for clarity.

Chart 2

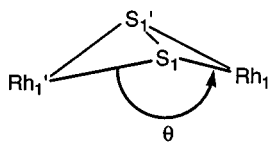

	Dihedral Angle θ (°)	Rh-Rh' Distance (A)
4a	108.23	2.980

wavenumbers (1965−1975 cm^{-1}) than for **4** (1984−1994 cm^{-1}), in keeping with greater electron density on the metal being available in the former for back-bonding to

Scheme 4. Direct Synthesis of Dinuclear Metal Complexes 4[a]

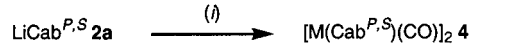

[a] Legend: (*i*) $^1/_2$[Mu(μ-Cl)$(CO)_2]_2$ (M = Rh, Ir), THF, 25 °C.

Scheme 5. Ligand Substitutions of 4[a]

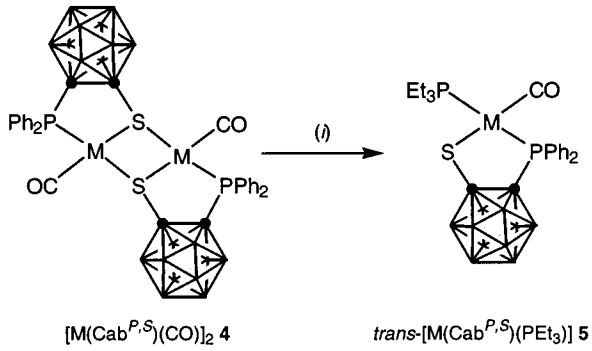

[a] Legend: (*i*) PEt_3, toluene, 25 °C.

CO. The structure of **5a**, determined by X-ray diffraction (Figure 5), is in agreement with the solution structure derived from other spectroscopic data: the two phosphorus atoms are in trans positions.

The average Rh−S distance of 2.370 Å is typical for other rhodium(I) thiolates.[18c] The two Rh−P distances are slightly different: 2.298(1) Å for the Rh−PPh_2 distance in the chelate and 2.317(2) Å for the Rh−PEt_3 distance. This difference may be interpreted in terms of the increased trans influence and the stronger bond of the diphenylphosphine group in the chelate compared to triethylphosphine.

Reaction of LiCab^{CH2P,S} (2b) with [Rh(CO)$_2$(acac)] (acac = Acetylacetonate). The direct reaction of [Rh$(CO)_2$(acac)] with 1 equiv of LiCab^{CH2P,S} (**2b**) in

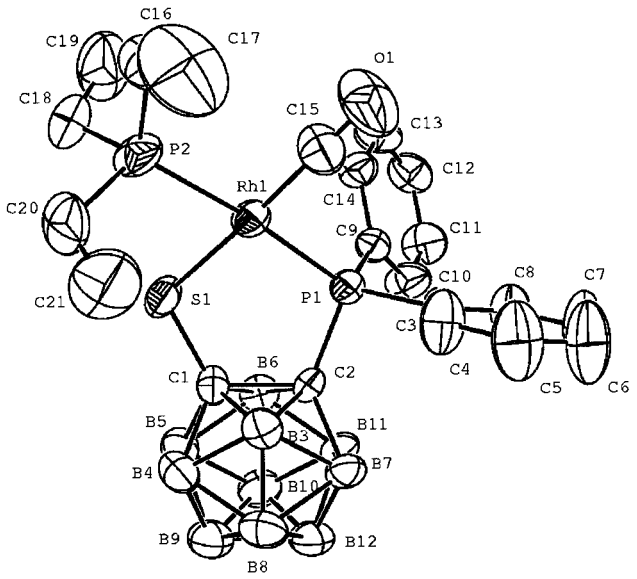

Figure 5. Molecular structure of **5a** with atom labeling. Ellipsoids show 30% probability levels; the unlabeled atoms are carbon atoms, and hydrogen atoms have been omitted for clarity.

THF afforded the dinuclear P,S-chelated phosphinothiolato metal complexes **6** in low yield (eq 1).

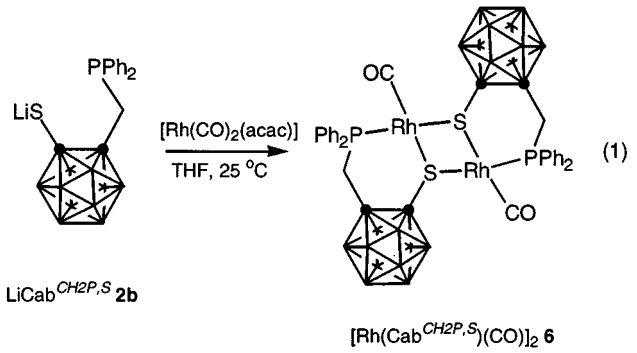

Complexes **6** were isolated as air-stable microcrystalline solids and were spectroscopically characterized. The composition of the new complexes **6** is unequivocally established by elemental analysis. Furthermore, the spectroscopic data (^{1}H, ^{13}C, and ^{31}P NMR) associated with **6** are also consistent with their assigned structures. Indeed, the ^{1}H NMR spectrum consists of multiplets from the $-PPh_2$ resonances (at around δ 7.56−7.80) and a doublet for the PCH_2 protons δ 3.45 ($^2J_{P-H} = 9$ Hz) in **6**. The ^{13}C NMR spectra have signals for complex **6**, three for the unique $-PPh_2$ carbons, one for the PCH_2 group, and one signal attributable to the carbonyl ligand. The pattern and relative intensity of the ν(CO) band of **6** resemble closely those of the compound having the dinuclear phosphinothiolato metal carbonyl environments. The phosphorus NMR spectra of **6** show a doublet resonance at δ 45.19 ($^1J_{Rh-P} = 157$ Hz), corresponding to the equivalent $-PPh_2$ groups placed trans to the bridging sulfur. For the rhodium complexes **4**−**7**, the coupling constants $^1J_{Rh-P}$ have higher values in the dinuclear complexes than in the mononuclear ones (for example, $^1J_{Rh-P}$ is 157−169 Hz for complexes **4a** and **6** and 128−133 Hz for complex **5a** and **7**), which indicates that the Rh−P bond of the chelating phosphinothiolate

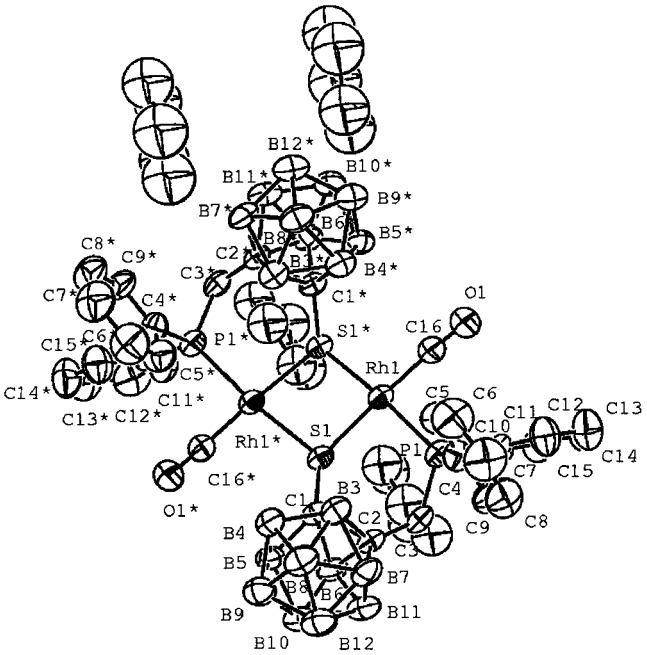

Figure 6. Molecular structure of **6**·4THF with atom labeling. Ellipsoids show 30% probability levels; the unlabeled atoms are carbon atoms, and hydrogen atoms have been omitted for clarity.

is strengthened. This, in turn, can be related to the weakening of the Rh−S bond due to bridge coordination.[23] The ^{31}P chemical shifts are displaced toward higher frequencies by 36.25 ppm compared to the five-membered-ring-containing complexes **4a**, in which δ_P 81.44, but these displacements are consistent with the dependency of the phosphorus chemical shifts with ring size and bond angles around phosphorus, an effect documented in diphosphine complexes.[24]

The crystal structure of **6**, which included THF molecules in a slow crystallization process, was determined by X-ray diffraction (Figure 6). Dinuclear complex **6** can be viewed as two Rh(Cab^{CH2P,S})(CO) fragments that have dimerized at an angle to give rise to the folded-parallelogram-shaped Rh_2S_2 center. The chelate angle P−Rh−S in the Rh(Cab^{CH2P,S}) six-membered ring of **6** is larger (95.01(6)°) than the corresponding chelate angle of 91.11(9)° (average) in the five-membered ring of Rh(Cab^{P,S}) in **4a** (Figure 3). The molecule has noncrystallographic C_2 symmetry. There are two longer Rh−S distances of 2.388(2) Å integrated in the chelate ring that are trans to carbonyl ligands and two shorter Rh−S distances of 2.383(2) Å that are trans to phosphorus.

The geometry of this complex **6** shows a hinged structure with a rather large dihedral angle between the two Rh,S,S planes. The hinged angle is smallest for the complex with the rhodium complex, **4a** (108,23°), and increases up to a value of 140.82° for the rhodium

(23) (a) Forniés-Cámer, J.; Masdeu-Bultó, A. M.; Claver, C.; Cardin, C. J. *Inorg. Chem.* **1998**, *37*, 2626. (b) Fazlur-Rahnam, A. K.; Verkade, J. G. *Inorg. Chem.* **1992**, *31*, 969. (c) Rauchfuss, T. B.; Shu, J. S.; Roundhill, D. M. *Inorg. Chem.* **1976**, *15*, 2096. (d) Rauchfuss, T. B.; Roundhill, D. M. *J. Am. Chem. Soc.* **1975**, *97*, 3386.

(24) (a) Lindner, E.; Fawzi, R.; Meyer, H. A.; Eichele, K.; Hiller, W. *Organometallics* **1992**, *11*, 1033. (b) Crumbliss, A. L.; Topping, R. J. In *Phosphorus-31 NMR Spectroscopy in Spectrochemical Analysis*; Verkade, J. G., Quin, L. D., Eds.; VCH: Weinheim, Germany, 1987; p 531. (c) Garrou, P. E. *Chem. Rev.* **1981**, *81*, 229.

complex **6**. Consequently, the metal−metal separation changes with the variation in the dihedral angle. It is smallest for the complex **4a** (2.980 Å) and increases up to a value of 3.4829 Å. The Rh−Rh distance, 3.4829 Å, indicates that these two metals are not bound directly to each other (typically 2.6−2.8 Å in dinuclear Rh(II) complexes).[18c,f]

Ligand Substitutions of 6. Treatment of dinuclear complex **6** with 2 equiv of PEt_3 in toluene afforded the corresponding mononuclear metal chelates [*trans*-Rh(Cab^{CH2P,S})(CO)(PEt_3)] (**7**), as shown in eq 2. The value

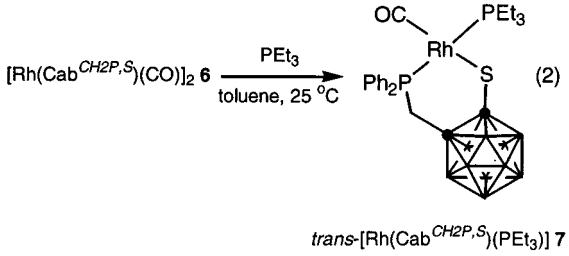

for the carbonyl stretch at 1972 cm^{-1} indicates a higher electron density on the rhodium center than that in **6** (2048 cm^{-1}) but is comparable to that in **5** (1965−1975 cm^{-1}). The absorption of the CO stretching vibration was shifted, due to the formation of the mononuclear complex **7**, which confers greater electron density to the metal. The PCH_2 protons of the phosphinomethyl tether gives in the ^{1}H NMR spectrum a doublet at δ 3.52 with a coupling constant $^2J_{P-H}$ of 9 Hz. The phosphorus NMR spectrum of **7** exhibits sharp signals at δ 88.54, corresponding to the $-PPh_2$ group of the chelate phosphinothiolate ligand, and at δ 26.22, corresponding to the PEt_3 ligand. The coupling constant $^2J_{P-P}$ = 316 Hz is typical of a trans-P,P arrangements that places the bulky $-PPh_2$ and PEt_3 groups away from each other, analogous to complexes **5**.

Catalytic Carbonylation of Methanol. A methanol carbonylation catalyst containing a diphosphine monosulfide ligand was recently described.[25] More recently, Dilworth et al. have published that dinuclear dithiolato rhodium complexes are readily available from a phosphinothiol ligand and are active carbonylation catalysts.[3] However, the use of *o*-carboranyl phosphinothiolate to induce a carbonylation reaction has no precedent so far. Thus, the catalytic activities of the bimetallic complexes **4** were tested for the carbonylation of methanol and were compared with those of the mononuclear complexes **5** under the same conditions. Figure 7 shows the reaction profiles for the various rhodium and iridium complexes by plotting the quantity of carbon monoxide consumed vs time, and Table 4 lists the turnover numbers. As a control experiment, the catalytic reaction was carried out with the Monsanto catalyst $[RhI_2(CO)_2]^-$, which was formed in situ from the added $[RhCl(CO)_2]_2$ under the stated reaction conditions. As can be seen in Figure 7 and Table 4, at equivalent rhodium catalyst concentrations, the dinuclear metal complex **4a** exhibits significant catalytic activity over the Monsanto catalyst. The increased catalytic activity of **4a** is most likely a consequence of the formation of the thermally stable

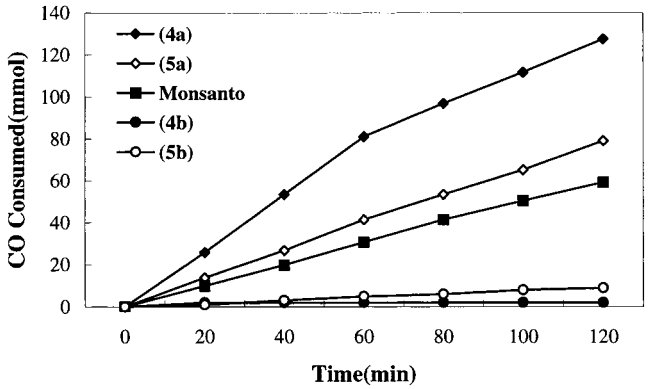

Figure 7. Carbonylation of methanol with various Rh and Ir complexes. Conditions: CH_3OH, 9.0 g; CH_3COOH, 20.0 g; CH_3I, 2.0 g; catalyst (1) **4a**, **4b** (0.025 mmol), (2) **5a**, **5b** (0.05 mmol); P = 700 psig, T = 180 °C.

Table 4. Maximum Turnover Numbers Observed during Methanol Carbonylation[a]

catalyst	max. turnover/h^{-1}	catalyst	max. turnover/h^{-1}
Monsanto	590	**4b**	20
4a	1280	**5b**	90
5a	790		

[a] Conditions as for Figure 7.

metal chelate that is imposed by the bulky *o*-carborane ligand backbone. The ^{31}P NMR spectrum of the inorganic residue remaining after the carbonylation reaction by **4a** indicates that a high proportion of the phosphorus remains bound to the rhodium center and retains the original bimetallic structure, as deduced from the chemical shift and coupling constant. The activity of the mononuclear rhodium complex **5a** is found to be comparable to that of the Monsanto catalyst even though **5a** is less active, by a factor of 2, than the corresponding dinuclear rhodium complex **4a**. In contrast to the rhodium complexes **4a** and **5a**, the iridium complexes **4b** and **5b** show extremely low activities.

Conclusion

Phosphinothiolato ligands **2** are representative of a series of easily accessible chelating ligands in which the two heteroatoms can be independently introduced in consecutive synthetic steps. Such a preparation warrants great flexibility, and the approach should allow fine-tuning of the ligands, with respect to both their steric and electronic properties, to form thiolato-bridged dinuclear species. Therefore, the results presented for complexes **4** and **6** are the first detailed structural studies of a P,S-chelating *o*-carboranyl phosphinothiolate with intramolecular coordination, and they nicely demonstrate the variety of dinuclear coordinations possible with P,S-chelating phosphinothiolato ligands. In Table 4, we offer the first data on the evaluation of *o*-carboranyl phosphinothiolato complexes of group 9 metals as precursors in the reaction of catalytic carbonylation of methanol with CO. The structurally characterized complexes **4** and **5** were tested.

Experimental Section

General Procedures. All manipulations were performed under a dry, oxygen-free, nitrogen or argon atmosphere using

(25) (a) Baker, M. J.; Giles, M. F.; Orpen, A. G.; Taylor, M. J.; Watt, R. J. *J. Chem. Soc., Chem. Commun.* **1995**, 197. (b) Eur. Pat. Appl. 632,006, 1994; *Chem. Abstr.* **1995**, *122*, 16406.

standard Schlenk techniques or in a Vacuum Atmospheres HE-493 drybox. THF was freshly distilled over potassium benzophenone. Toluene was dried and distilled from sodium benzophenone. Dichloromethane and hexane were dried and distilled over CaH_2. ^{13}C, ^{1}H, and ^{31}P NMR spectra were recorded on a Varian Gemini 2000 spectrometer operating at 50.3, 200.1, and 80.0 MHz, respectively. All proton and carbon chemical shifts were measured relative to internal residual benzene from the lock solvent (99.5% C_6D_6) and then referenced to Me_4Si (0.00 ppm). The ^{31}P NMR spectra were recorded with 85% H_3PO_4 as an external standard. IR spectra were recorded on a Biorad FTS-165 spectrophotometer. Elemental analyses were performed with a Carlo Erba Instruments CHNS-O EA1108 analyzer. All melting points were uncorrected. Decaborane and *o*-carborane were purchased from Katechem and used without purification. [Rh(μ-Cl)$(CO)_2]_2$, [Ir(μ-Cl)$(CO)_2]_2$, and [Rh$(CO)_2$(acac)] were purchased from Strem Chemical and used as received. The following starting materials were prepared according to literature procedures: CabH^P (**1a**),[12] CabH^{CH2P} (**1b**),[13] [Rh(μ-Cl)(cod)$]_2$,[26] and [Ir(μ-Cl)(cod)$]_2$.[27]

Preparation of [Rh(Cab^{P,S})(cod)] (3a). To Hcab^P (**1a**; 0.99 g, 3.0 mmol) dissolved in hexane (20 mL) at −10 °C was added a solution of Bu^{n}Li in hexane (3.0 mmol). The resulting mixture was stirred for 12 h at room temperature. The white precipitate formed was separated from the solution by decantation. The solid LiCab^P was washed twice with 30 mL of pentane and dried in vacuo; yield 0.97 g (2.9 mmol, 97%). LiCab^P (0.33 g, 1.0 mmol) dissolved in THF (30 mL) was slowly added to a suspension of sublimed sulfur (0.035 g, 1.1 mmol) in THF (20 mL) at −78 °C. The solution was warmed to room temperature, and [Rh(μ-Cl)(cod)$]_2$ (0.247 g, 0.5 mmol) was added. The reaction mixture was then allowed to react at 0 °C for 1 h, and the solution was stirred for another 2 h at room temperature. The solution gradually turned dark brown, suggesting the formation of a phosphinothiolato metal complex. The solution was reduced in vacuo to about half its original volume, and some insoluble material was removed by filtration. The solvent was removed under vacuum, and the resulting residue was taken up in a minimum of methylene chloride and then transferred to a column of silica gel. The crude residue was purified by column chromatography, affording >95% pure complex as pure crystals. Yield: 0.49 g (0.86 mmol, 86%). Data for **3a** are as follows. Anal. Calcd for $C_{22}H_{32}B_{10}PSRh$: C, 46.31; H, 5.65. Found: C, 46.40; H, 5.72. IR (KBr, cm^{-1}): ν(B−H) 2606, 2572, 2560; ν(C═C), 1437. ^{1}H NMR (200.13 MHz, ppm, $CDCl_3$): 8.07 (m, PPh_2), 7.55 (m, PPh_2), 5.25 (br, 4H, ═C*H* cod), 2.94 (br, 4H, CH_{exo} cod), 2.32 (br, 4H, CH_{endo} cod). $^{13}C\{^{1}H\}$ NMR (50.3 MHz, ppm, $CDCl_3$): 134.11, 133.85, 130.46, 126.96, 126.75 (s, PPh_2), 100.49 (s, ═*C*H cod), 77.80 (s, C_2B_{10}), 30.49, 27.55 (s, *C*H cod). $^{31}P\{^{1}H\}$ NMR (80.0 MHz, ppm, $CDCl_3$): 81.46 (d, $^{1}J_{Rh-P}$ = 169 Hz, *P*Ph_2).

Preparation of [Ir(Cab^{P,S})(cod)] (3b). A solution of freshly prepared LiCab^{P,S} (**2a**; 0.37 g, 1.0 mmol) in THF (30 mL) was added over 1 h to a suspension of [Ir(μ-Cl)(cod)$]_2$ (0.34 g, 0.5 mmol) in toluene (20 mL) at −78 °C. The reaction mixture was stirred for 12 h at room temperature, after which the suspended solid was collected by filtration. The solution was further reduced in vacuo to about half its original volume, and some insoluble material was removed by filtration. The solvent was removed under vacuum, and the resulting residue was taken up in a minimum of methylene chloride and then transferred to a column of silica gel. The crude residue was purified by column chromatography, affording >95% pure complex as pure crystals. Colorless crystals of **3b** were formed in 79% yield (0.52 g, 0.79 mmol). Data for **3b** are as follows. Anal. Calcd for $C_{22}H_{32}B_{10}PSIr$: C, 40.05; H, 4.89. Found: C, 40.09; H, 4.94. IR (KBr, cm^{-1}): ν(B−H) 2604, 2573, 2561; ν(C═C), 1439. ^{1}H NMR (200.13 MHz, ppm, $CDCl_3$): 8.00 (m, PPh_2), 7.55 (m, PPh_2), 4.98 (br, 4H, ═C*H* cod), 2.36 (br, 4H, CH_{exo} cod), 2.18 (br, 4H, CH_{endo} cod). $^{13}C\{^{1}H\}$ NMR (50.3 MHz, ppm, $CDCl_3$): 136.88, 135.43, 131.19, 128.33, 127.11 (s, PPh_2), 106.01 (s, ═*C*H cod), 83.46 (s, C_2B_{10}), 36.28, 30.23 (s, *C*H cod). $^{31}P\{^{1}H\}$ NMR (80.0 MHz, ppm, $CDCl_3$): 83.19 (s, *P*Ph_2).

Synthesis of [Rh(Cab^{P,S})(CO)]$_2$ (4a). A solution of complex **3a** (0.29 g, 0.5 mmol) in toluene (20 mL) was treated with excess CO gas for 5 min at room temperature. The orange color of the solution quickly faded to give a yellow solution. The volatile substances were then removed in vacuo, and the resulting solid was extracted with methylene chloride. Addition of hexane to the concentrated extract gave complex **4a** as yellow crystals. Yield: 0.23 g (0.23 mmol, 93%). Data for **4a** are as follows. Anal. Calcd for $C_{30}H_{40}B_{20}O_2P_2S_2Rh_2$: C, 36.74; H, 4.11. Found: C, 36.77; H, 4.18. IR (KBr, cm^{-1}): ν(B−H) 2577; ν(C═O), 1994; ν(C═C), 1437. ^{1}H NMR (200.13 MHz, ppm, $CDCl_3$): 8.43 (br, PPh_2), 7.66 (br, PPh_2). $^{13}C\{^{1}H\}$ NMR (50.3 MHz, ppm, $CDCl_3$): 185.90 (d, $^{1}J_{Rh-C}$ = 57 Hz, *C*O), 136.04−126.71 (s, PPh_2), 94.00 (s, C_2B_{10}), 94.00 (s, $^{1}J_{P-C}$ = 12 Hz, C_2B_{10}). $^{31}P\{^{1}H\}$ NMR (80.0 MHz, ppm, $CDCl_3$): 81.44 (d, $^{1}J_{Rh-P}$ = 169 Hz, *P*Ph_2).

Synthesis of [Ir(Cab^{P,S})(CO)]$_2$ (4b). A procedure analogous to the preparation of **4a** was used, but with **3b** (0.33 g, 0.5 mmol) in toluene as the starting material. Thus, **4b** was crystallized from a methylene chloride and hexane mixture. Yield: 0.25 g (0.22 mmol, 88%). Data for **4b** are as follows. Anal. Calcd for $C_{30}H_{40}B_{20}O_2P_2S_2Ir_2$: C, 31.08; H, 3.48. Found: C, 31.11; H, 3.52. IR (KBr, cm^{-1}): ν(B−H) 2580; ν(C═O), 1984; ν(C═C), 1433. ^{1}H NMR (200.13 MHz, ppm, $CDCl_3$): 8.39 (br, PPh_2), 7.65 (br, PPh_2). $^{13}C\{^{1}H\}$ NMR (50.3 MHz, ppm, $CDCl_3$): 206.10 (s, *C*O), 132.99, 131.98, 128.03 (s, PPh_2), 79.53 (s, C_2B_{10}). $^{31}P\{^{1}H\}$ NMR (80.0 MHz, ppm, $CDCl_3$): 53.18 (s, *P*Ph_2).

Reaction of 2a with [Rh(μ-Cl)$(CO)_2]_2$. A 0.37 g amount of **2a** (1.0 mmol) was dissolved in 20 mL of dry THF and cooled to −10 °C. A 0.19 g amount of [Rh(μ-Cl)$(CO)_2]_2$ (0.5 mmol) was added with stirring over 30 min, and the solution was warmed to room temperature. The yellow solution turned dark orange as the solution was warmed. The solution was filtered in air, and the solvent was removed under reduced pressure. The remaining solid was passed through a short column of silica gel with CH_2Cl_2 as the eluent. A 0.38 g amount of **4a** was obtained after removal of the solvent (0.39 mmol, 78% yield).

Reaction of 2a with [Ir(μ-Cl)$(CO)_2]_2$. A similar procedure was employed as described above, but with the following quantities: **2a** (0.37 g, 1.0 mmol); [Ir(μ-Cl)$(CO)_2]_2$ (0.28 g, 1.0 mmol). A yellow solid of **4b** was isolated as described for the rhodium complex **4a**. Yield: 0.38 g (0.33 mmol, 66%).

Reaction of 4a with PEt$_3$. A solution of complex **4a** (0.20 g, 0.2 mmol) in toluene (10 mL) was treated with PEt_3 (0.09 mL, 0.6 mmol) at room temperature for 1 h. The orange color of the solution quickly faded to give a brown-yellow solution. The NMR spectra of this sample showed complete conversion to *trans*-[Rh(Cab^{P,S})(CO)(PEt_3)] (**5a**). The volatile substances were then removed in vacuo, and the resulting solid was extracted with methylene chloride. The addition of hexane to the concentrated extract gave complex **5a** as yellow crystals. Yield: 0.20 g (0.33 mmol, 83%). Data for **5a** are as follows. Anal. Calcd for $C_{21}H_{35}B_{10}OP_2SRh$: C, 41.45; H, 5.80. Found: C, 41.50; H, 5.88. IR (KBr, cm^{-1}): ν(B−H) 2596; ν(C═O), 1975. ^{1}H NMR (200.13 MHz, ppm, $CDCl_3$): 8.26 (m, PPh_2), 7.54 (m, PPh_2), 1.85 (dq, 6, PCH_2), 1.20 (dt, 9, PCH$_2$*Me*). $^{13}C\{^{1}H\}$ NMR (50.3 MHz, ppm, $CDCl_3$): 187.11 (d, $^{1}J_{Rh-C}$ = 58 Hz, *C*O), 134.61, 130.43, 126.82 (s, PPh_2), 16.45 (d, $^{1}J_{P-C}$ = 13 Hz, P(*C*H$_2$Me)$_3$), 6.93 (s, P(CH$_2$*Me*)$_3$). $^{31}P\{^{1}H\}$ NMR (80.0 MHz, ppm, $CDCl_3$): 82.21 (dd, $^{2}J_{P-P}$ = 294 Hz, $^{1}J_{Rh-P}$ = 133 Hz, *P*Ph_2), 26.22 (dd, $^{2}J_{P-P}$ = 294 Hz, $^{1}J_{Rh-P}$ = 124 Hz, *P*Et_3).

Reaction of 4b with PEt$_3$. A procedure similar to that described above was employed, but with the following quanti-

(26) Giordano, G.; Crabtree, R. H. *Inorg. Synth.* **1979**, *19*, 218.
(27) Herde, J. L.; Lambert, J. C.; Senoff, C. V. *Inorg. Synth.* **1974**, *15*, 18.

ties: **4b** (0.23 g, 0.2 mmol); PEt_3 (0.09 mL, 0.6 mmol). A yellow solid of *trans*-[Ir(Cab^{P,S})(CO)(PEt_3)] (**5b**) was isolated as described for the rhodium complex **5a**: isolated yield 0.21 g (0.3 mmol), 75%. Data for **5b** are as follows. Anal. Calcd for $C_{21}H_{35}B_{10}OP_2SIr$: C, 36.14; H, 5.06. Found: C, 36.19; H, 5.10. IR (KBr, cm^{-1}): ν(B−H) 2577; ν(C═O), 1965. ^{1}H NMR (200.13 MHz, ppm, $CDCl_3$): 8.20 (br, 5, P*Ph*$_2$), 7.55 (br, 5, P*Ph*$_2$), 2.00 (dq, 6, PC*H*$_2$), 1.18 (dt, 9, PCH$_2$*Me*). ^{13}C{^{1}H} NMR (50.3 MHz, ppm, $CDCl_3$): 206.10 (s, *C*O), 136.54, 132.27, 128.34 (s, P*Ph*$_2$), 18.31 (d, $^1J_{P-C}$ = 34 Hz, P(*C*H$_2$Me)$_3$), 8.52 (s, P(CH$_2$*Me*)$_3$). ^{31}P-{^{1}H} NMR (80.0 MHz, ppm, $CDCl_3$): 79.60 (d, $^2J_{P-P}$ = 130 Hz, *P*Ph$_2$), 23.12 (d, $^2J_{P-P}$ = 130 Hz, *P*Et$_3$).

Preparation of [Rh(Cab^{CH2P,S})(CO)]$_2$ (6). To Hcab^{CH2P} (**1b**; 1.03 g, 3.0 mmol) dissolved in hexane (20 mL) at −10 °C was added a solution of Bu^{n}Li in hexane (3.0 mmol). The resulting mixture was stirred for 12 h at room temperature. The white precipitate formed was separated from the solution by decantation. The solid LiCab^{CH2P} was washed twice with 30 mL of pentane and dried in vacuo; yield 1.01 g (2.9 mmol, 97%). LiCab^{CH2P} (0.35 g, 1.0 mmol) dissolved in THF (30 mL) was slowly added to a suspension of sublimed sulfur (0.035 g, 1.1 mmol) in THF (20 mL) at −78 °C. The solution was warmed to room temperature, and Rh(CO)$_2$(acac) (0.26 g, 1.0 mmol) was added. The reaction mixture was then allowed to react at 0 °C for 1 h, and the solution was stirred for another 2 h at room temperature. The solution gradually turned dark brown, suggesting the formation of a phosphinothiolato metal complex. The solution was reduced in vacuo to about half its original volume, and some insoluble material was removed by filtration. The solvent was removed under vacuum, and the resulting residue was taken up in a minimum of methylene chloride and then transferred to a column of silica gel. The crude residue was purified by column chromatography, affording >95% pure complex as pure crystals. Yield: 0.21 g (0.21 mmol, 42%). Data for **6** are as follows. Anal. Calcd for $C_{32}H_{44}B_{20}O_2P_2S_2Rh_2$: C, 38.10; H, 4.40. Found: C, 38.17; H, 4.51. IR (KBr, cm^{-1}): ν(B−H) 2591; ν(C═O), 2048, 1982. ^{1}H NMR (200.13 MHz, ppm, $CDCl_3$): 7.80 (m, P*Ph*$_2$), 7.56 (m, P*Ph*$_2$), 3.45 (d, $^2J_{P-H}$ = 9 Hz, PC*H*$_2$). ^{13}C{^{1}H} NMR (50.3 MHz, ppm, $CDCl_3$): 227.82 (d, $^1J_{Rh-C}$ = 57 Hz, *C*O), 133.36, 131.32, 129.07 (s, P*Ph*$_2$), 29.65 (d, $^1J_{P-C}$ = 12 Hz, P*C*H$_2$). ^{31}P{^{1}H} NMR (80.0 MHz, ppm, $CDCl_3$): 45.19 (d, $^1J_{Rh-P}$ = 157 Hz, *P*Ph$_2$).

Reaction of 6 with PEt$_3$. A solution of complex **6** (0.2 g, 0.2 mmol) in toluene (10 mL) was treated with PEt_3 (0.06 mL, 0.4 mmol) at room temperature for 1 h. The orange color of the solution quickly faded to give a brown-yellow solution. The NMR spectra of this sample showed complete conversion to *trans*-[Rh(Cab^{CH2P,S})(CO)(PEt_3)] (**7**). The volatile substances were then removed in vacuo, and the resulting solid was extracted with methylene chloride. The addition of hexane to the concentrated extract gave complex **7** as yellow crystals. Yield: 0.16 g (0.26 mmol, 64%). Data for **7** are as follows. Anal. Calcd for $C_{22}H_{37}B_{10}OP_2SRh$: C, 42.45; H, 5.99. Found: C, 42.48; H, 6.04. IR (KBr, cm^{-1}): ν(B−H) 2587; ν(C═O), 1972; ν(P−C), 1385. ^{1}H NMR (200.13 MHz, ppm, $CDCl_3$): 7.74 (m, P*Ph*$_2$), 7.49 (m, P*Ph*$_2$), 3.52 (d, $^2J_{P-H}$ = 9 Hz, PC*H*$_2$), 1.91 (dq, 6, PC*H*$_2$), 1.17 (dt, 9, PCH$_2$*Me*). ^{13}C{^{1}H} NMR (50.3 MHz, ppm, $CDCl_3$): 198.09 (d, $^1J_{Rh-C}$ = 58 Hz, *C*O), 133.34, 130.93, 128.93 (s, P*Ph*$_2$), 34.73 (d, $^1J_{P-C}$ = 21 Hz, PPh$_2$*C*H$_2$), 16.47 (d, $^1J_{P-C}$ = 25 Hz, P(*C*H$_2$Me)$_3$), 6.47 (s, P(CH$_2$*Me*)$_3$). ^{31}P{^{1}H} NMR (80.0 MHz, ppm, $CDCl_3$): 88.54 (dd, $^2J_{P-P}$ = 316 Hz, $^1J_{Rh-P}$ = 128 Hz, *P*Ph$_2$), 26.22 (dd, $^2J_{P-P}$ = 316 Hz, $^1J_{Rh-P}$ = 120 Hz, *P*Et$_3$).

General Procedure for Catalytic Experiments. A solution of the catalyst (0.05 mmol), methanol (9.0 g), acetic acid (20.0 g), and methyl iodide (2.0 g) in dried solvent (20.0 g) was stirred in an autoclave under a constant carbon monoxide pressure (700 psgi) at 180 °C, for 120 min. The drop in CO pressure in the ballast (reservoir) tank (500 mL) equipped with a high-pressure regulator and a pressure transducer was recorded by means of a recorder, which provides a convenient method for observing the progress of the reaction. After the required reaction time, the autoclave was cooled to room temperature, the pressure was carefully released, and the solution was passed through Celite and analyzed by GC, GC-MS, and ^{1}H NMR spectroscopy. Conversions were determined by GC.

X-ray Crystallography. Suitable crystals of **3a**, **3b**, **4a**·(hexane), **4b**, **5a**, and **6**·4THF were obtained by slow diffusion of hexane into a methylene chloride solution of the complexes at room temperature and were mounted on glass fibers. Crystal data and experimental details are given in Table 1. The data sets for **3a**, **3b**, **4a**·(hexane), **4b**, **5a**, and **6**·4THF were collected on an Enraf CAD4 automated diffractometer. Mo Kα radiation (λ = 0.7107 Å) was used for all structures. Each structure was solved by the application of direct methods using the SHELXS-96 program[28a] and least-squares refinement using SHELXL-97.[28b] All non-hydrogen atoms in compounds **3a**, **3b**, **4a**·(hexane), **4b**, **5a**, and **6**·4THF were refined anisotropically. All other hydrogen atoms were included in calculated positions.

Acknowledgment. We wish to acknowledge the financial support of the Korea Research Foundation made in the program year of 2001 (Grant No. 2001-041-D00119).

Supporting Information Available: Tables of crystallographic data (excluding structure factors) for the structures of **3a**, **3b**, **4a**·(hexane), **4b**, **5a**, and **6**·4THF, as well as data in CIF format. This material is available free of charge via the Internet at http://pubs.acs.org. These data have also been deposited with the Cambridge Crystallographic Data Centre as supplementary publication nos. CCDC-169164 (**3a**), CCDC-169163 (**3b**), CCDC-169161 (**4a**·(hexane)), CCDC-169165 (**4b**), CCDC-169162 (**5a**), and CCDC-169166 (**6**·4THF). Copies of the data can be obtained free of charge on application to the CCDC, 12 Union Road, Cambridge CB2 1EZ, U.K. (fax, (+44) 1223-336-033; e-mail, deposit@ccdc.cam. ac.uk).

OM0107789

(28) (a) Sheldrick, G. M. *Acta Crystallogr. Sect. A* **1990**, *46*, 467. (b) Sheldrick, G. M. SHELXL, Program for Crystal Structure Refinement; University of Göttingen, Göttingen, Germany, 1997.